CHEMISTRY
AN ASIAN JOURNAL
ACES
FULL PAPER

DOI: 10.1002/asia.201300327

2,3-Di(2-pyridyl)-5-phenylpyrazine: A NN-CNN-Type Bridging Ligand for Dinuclear Transition-Metal Complexes

Si-Hai Wu,[a, b] Yu-Wu Zhong,*[a, c] and Jiannian Yao[a]

Abstract: A new bridging ligand, 2,3-di(2-pyridyl)-5-phenylpyrazine (dpppzH), has been synthesized. This ligand was designed so that it could bind two metals through a NN-CNN-type coordination mode. The reaction of dpppzH with *cis*-[(bpy)$_2$RuCl$_2$] (bpy = 2,2′-bipyridine) affords monoruthenium complex [(bpy)$_2$Ru(dpppzH)]$^{2+}$ (**1**$^{2+}$) in 64% yield, in which dpppzH behaves as a NN bidentate ligand. The asymmetric biruthenium complex [(bpy)$_2$Ru(dpppz)Ru(Mebip)]$^{3+}$ (**2**$^{3+}$) was prepared from complex **1**$^{2+}$ and [(Mebip)RuCl$_3$] (Mebip = bis(*N*-methylbenzimidazolyl)pyridine), in which one hydrogen atom on the phenyl ring of dpppzH is lost and the bridging ligand binds to the second ruthenium atom in a CNN tridentate fashion. In addition, the RuPt heterobimetallic complex [(bpy)$_2$Ru(dpppz)Pt(C≡CPh)]$^{2+}$ (**4**$^{2+}$) has been prepared from complex **1**$^{2+}$, in which the bridging ligand binds to the platinum atom through a CNN binding mode. The electronic properties of these complexes have been probed by using electrochemical and spectroscopic techniques and studied by theoretical calculations. Complex **1**$^{2+}$ is emissive at room temperature, with an emission λ_{max} = 695 nm. No emission was detected for complex **2**$^{3+}$ at room temperature in MeCN, whereas complex **4**$^{2+}$ displayed an emission at about 750 nm. The emission properties of these complexes are compared to those of previously reported Ru and RuPt bimetallic complexes with a related ligand, 2,3-di(2-pyridyl)-5,6-diphenylpyrazine.

Keywords: bridging ligands · coordination modes · cyclometalated complexes · platinum · ruthenium

Introduction

The design of polyazine bridging ligands for the construction of bimetallic or macromolecular coordination assemblies has received much attention.[1] A "good" bridging ligand should have a rigid and well-defined geometry and allow optimal orbital overlap between the metals and the organic ligands. Because of their appealing photophysical and electrochemical properties, the resulting bimetallic or multimetallic complexes have been extensively used in a wide range of fields, such as molecular electronics,[2] electrochromism,[3] and the photoconversion of solar energy.[4] One of the most extensively studied bridging ligands is 2,3,5,6-tetrakis(2-pyridyl)pyrazine (tppz, Scheme 1), which has been shown to yield a great number of linear and rigid molecular assemblies when bound to octahedral transition-metal ions in a NNN-NNN bis-tridentate fashion.[5] Another bridging ligand that

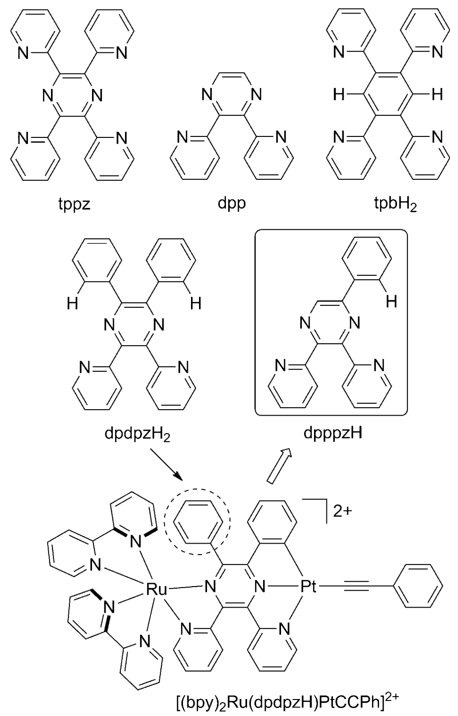

Scheme 1. Bridging ligands and the design of new ligand dpppzH.

---

[a] S.-H. Wu, Prof. Dr. Y.-W. Zhong, Prof. Dr. J. Yao
Beijing National Laboratory for Molecular Sciences
CAS Key Laboratory of Photochemistry
Institute of Chemistry, Chinese Academy of Sciences
Beijing 100190 (China)
E-mail: zhongyuwu@iccas.ac.cn
Homepage: http://zhongyuwu.iccas.ac.cn/

[b] S.-H. Wu
University of Chinese Academy of Sciences
Beijing 100049 (China)

[c] Prof. Dr. Y.-W. Zhong
State Key Laboratory of Coordination Chemistry
Nanjing University
Nanjing 210093 (China)

Supporting information for this article is available on the WWW under http://dx.doi.org/10.1002/asia.201300327.

has received extensive attention is 2,3-bis(2-pyridyl)pyrazine (dpp). This ligand binds to two metals through a NN-NN-type coordination mode and is particularly useful for the construction of macromolecular complexes with multiple metal centers.[6] Despite the progress in this area, the development of new polyazine bridging ligands with comparable and complementary electronic properties is still of great interest to the materials science and chemistry communities.[1]

Recently, there has been growing interest in the synthesis and study of cyclometalated complexes that contain a σ M−C bond.[7] These complexes either contain a CN-type bidentate ligand or a NCN/CNN-type tridentate chelate ligand. The most studied cyclometalated complexes have been those that bind to iridium,[8] ruthenium,[9] and platinum ions.[10] Because of the presence of the anionic carbon ligand, these complexes exhibit significantly different photophysical and electrochemical properties with respect to their corresponding noncyclometalated complexes. However, most of these studies have been concerned with monometallic complexes and the design of bridging ligands for the synthesis of cyclometalated dinuclear complexes has been limited. Some representative examples include NCN-NCN-type bis-cyclometalating ligands 1,2,4,5-tetra(pyrid-2-yl)benzene ($tpbH_2$, Scheme 1),[11] 1,3,6,8-tetra(pyrid-2-yl)pyrene,[12] and others.[13] These ligands have been used for the syntheses of bis-ruthenium complexes and for studies of metal−metal electronic coupling.

In addition to these above-mentioned bis-cyclometalating ligands, we recently reported that 2,3-di(2-pyridyl)-5,6-diphenylpyrazine ($dpdpzH_2$, Scheme 1) displayed rich coordination chemistry with various transition metals, such as ruthenium,[14] platinum,[15] and rhenium,[16] to yield a number of monometallic and bimetallic complexes with interesting electrochemical and spectroscopic properties. In the case of bimetallic complexes, the bridging ligand and the metal atoms can either connect through NN-NN, NN-CNN, or CNN-CNN-type coordination modes, depending on whether the two phenyl rings of $dpdpzH_2$ bind to the metal site or not. Among these compounds, one interesting example is the RuPt heterobimetallic complex $[(bpy)_2Ru(dpdpzH)PtC{\equiv}CPh]^{2+}$ (Scheme 1),[15] where bpy is 2,2′-bipyridine and dpdpz is the bis-deprotonated form of $dpdpzH_2$. This complex emits near-infrared (NIR) light[17] ($\lambda_{max} = 780$ nm) with a quantum yield (ϕ) of 0.15%, which is relatively higher than that of monoruthenium complex $[(bpy)_2Ru(dpdpzH_2)]^{2+}$, which emits at 709 nm ($\phi = 0.057\%$).[14] As a continuation of this project, we conjectured that the untouched phenyl ring of the bridging ligand in $[(bpy)_2Ru(dpdpzH)PtC{\equiv}CPh]^{2+}$ (Scheme 1, dashed circle) may rotate freely to provide a non-emissive deactivation pathway. Thus, a new ligand, 2,3-di(2-pyridyl)-5-phenylpyrazine (dpppzH), was designed in which this phenyl ring was removed. Herein, we describe the use of dpppzH as a NN-CNN-type bridging ligand for the synthesis of RuRu and RuPt bimetallic complexes and electrochemical and spectroscopic studies of these complexes. In addition, density functional theory (DFT) and time-dependent DFT (TDDFT) calculations have been performed to complement these experimental results.

Abstract in Chinese:

设计合成了一种新型桥联配体2,3-二(2-吡啶)-5-苯基吡嗪(dpppzH)。这种配体能够通过NN-CNN 类型配位模式和两个金属进行螯合。dpppzH 和*cis*-$[(bpy)_2RuCl_2]$反应生成NN 二齿配位单核化合物$[(bpy)_2Ru(dpppzH)]^{2+}$ (**1**$^{2+}$)。**1**$^{2+}$与$[(Mebip)RuCl_3]$反应得到不对称双钌配合物$[(bpy)_2Ru(dpppz)Ru(Mebip)]^{3+}$ (**2**$^{3+}$)，其中第二个金属钌以CNN 的配位模式与桥联配体结合。此外，从化合物**1**$^{2+}$出发，制备了Ru-Pt 异核配合物$[(bpy)_2Ru(dpppz)Pt(CCPh)]^{2+}$ (**4**$^{2+}$)。其中，金属铂以CNN 的配位方式与桥联配体结合。利用电化学、光谱以及理论计算等方法对这些配合物的光电性质进行了详细的研究。在室温条件下，配合物**1**$^{2+}$和**4**$^{2+}$最大发射波长在695 nm和750 nm 左右，配合物**2**$^{3+}$不发光。配合物**1**$^{2+}$和**4**$^{2+}$的发光量子产率和激发态寿命高于先前报道的基于桥联配体2,3-二(2-吡啶基)-5,6-二苯基吡嗪的类似物。

Results and Discussion

Synthesis and Characterization

The compounds that were studied herein are shown in Scheme 2. Ligand dpppzH was prepared by the condensation of D,L-phenylethylenediamine with 2,2′-pyridil, followed by subsequent dehydrogenation; D,L-phenylethylenediamine was prepared according to a literature procedure by the reduction of α-azidoacetophenone *O*-methyl oxime ether with lithium aluminum hydride.[18] The ^1H NMR spectrum of dpppzH shows a singlet at $\delta = 9.11$ ppm, which is assigned to the proton on the pyrazine ring. The reaction of dpppzH with *cis*-$[(bpy)_2RuCl_2]$, followed by anion exchange with KPF_6, gave monoruthenium complex $[(bpy)_2Ru(dpppzH)](PF_6)_2$ (**1**$^{2+}$) in 64% yield. The coordination mode between Ru and dpppzH was confirmed by subsequent transformations.

The treatment of complex **1**$^{2+}$ with $[(Mebip)RuCl_3]$[19] (Mebip = bis-(*N*-methylbenzimidazolyl)pyridine) in the presence of AgOTf afforded the asymmetric bis-ruthenium complex $[(bpy)_2Ru(dpppz)Ru(Mebip)](PF_6)_3$ (**2**$^{3+}$), where dpppz is the mono-deprotonated form of dpppzH. The identity of complex **2**$^{3+}$ was confirmed by mass spectroscopy, single-crystal X-ray diffraction, and electrochemical studies. The reaction of monoruthenium complex **1**$^{2+}$ with K_2PtCl_4 in a mixture of MeCN and water[10] gave the crude hetero-dinuclear $Ru^{II}Pt^{II}$ complex $[(bpy)_2Ru(dpppz)PtCl](PF_6)_2$ (**3**$^{2+}$) in good yield (90%); this crude product was used in a subsequent transformation without further purification. The reaction of complex **3**$^{2+}$ with phenylacetylene, in the presence of CuI and triethylamine,[20] afforded platinum-acetylide complex **4**$^{2+}$ in 70% yield. The successful synthesis and isolation

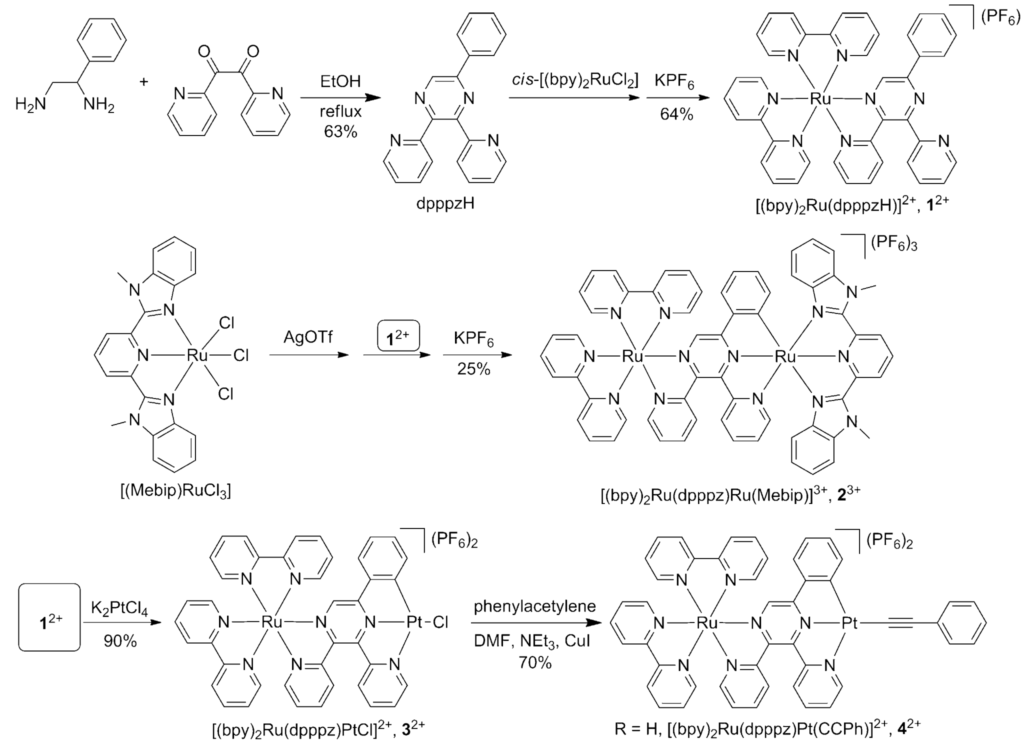

Scheme 2. Synthesis of the studied compounds.

of complexes $\mathbf{2}^{3+}$ and $\mathbf{4}^{2+}$ indicate that the [Ru(bpy)$_2$] component in complex $\mathbf{1}^{2+}$ binds to the NN side of dpppzH and, hence, that the open CNN side is available to accommodate another cyclometalated ion.

Single-Crystal Structures

A single crystal of complex [**2**](PF$_6$)$_3$ was obtained in a mixture of MeCN and Et$_2$O; the X-ray structure is shown in Figure 1.[21] Both ruthenium atoms adopt a distorted octahedral configuration. The Ru1 atom has a tris-bidentate coordination mode, whereas the Ru2 atom has a bis-tridentate coordination mode and is connected to the phenyl ring of the bridging ligand through a Ru−C bond. The two ruthenium atoms are separated by a Ru−Ru distance of 6.78 Å. The Ru−N bonds are associated with the noncyclometalated Ru1 atom and are within the range 2.04–2.06 Å. In many of the reported cyclometalated monoruthenium complexes,[19,22] the Ru−C bond is slightly shorter than the Ru−N bonds. However, the Ru2−C1 bond in complex $\mathbf{2}^{3+}$ has a distance of 2.02 Å, which is longer than the Ru2−N7 (1.96 Å) and Ru2−N10 bonds (1.99 Å). In addition, the Ru2−N8 bond (2.18 Å) is much longer relative to other Ru−N bonds, owing to the *trans* effect of the σ Ru2−C1 bond. The two planes of the pyridine groups with the N5 and N8 atoms have a torsion angle of 22.1°.

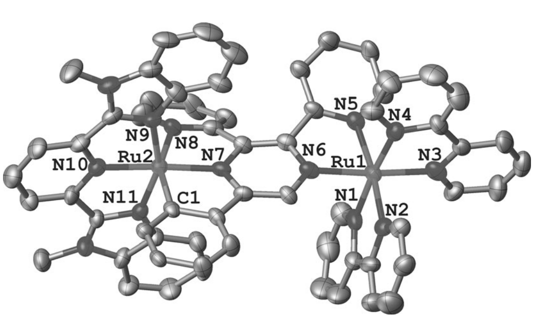

Figure 1. Single-crystal X-ray structure of complex [**2**](PF$_6$)$_3$; thermal ellipsoids are set at 30 % probability. Counteranions and hydrogen atoms are omitted for clarity. Selected bond lengths [Å]: Ru1–Ru2 6.78, Ru1–N1 = Ru1–N2 = Ru1–N5 = Ru1–N6 2.06, Ru1–N3 2.05, Ru1–N4 2.04, Ru2–C1 2.02, Ru2–N7 1.96, Ru2–N8 2.18, Ru2–N9 2.06, Ru2–N10 1.99, Ru2–N11 2.05.

Electrochemical Studies

The cyclic voltammograms (CVs) of these complexes are shown in Figure 2. The corresponding electrochemical data are summarized in Table 1, together with those of some related complexes for comparison. The anodic scan of monoruthenium complex $\mathbf{1}^{2+}$ shows one Ru$^{II/III}$ redox couple at +1.41 V versus Ag/AgCl, which is comparable to those of [(bpy)$_2$Ru(dpp)]$^{2+}$ and [(bpy)$_2$Ru(dpdpzH$_2$)]$^{2+}$.[14] Four cathodic waves for complex $\mathbf{1}^{2+}$ appear at −0.96, −1.43, −1.64, and −1.98 V. The first wave at −0.96 V is assigned to the reduction of the dpppzH ligand;[14] the other three waves cannot be clearly assigned. However, two of these waves must be associated with the reductions of two bpy ligands. The further reduction of dpppzH ligand may be responsible for the remaining wave.

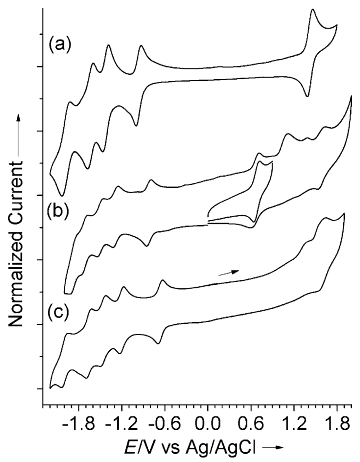

Figure 2. CVs of a) $\mathbf{1}^{2+}$, b) $\mathbf{2}^{3+}$, and c) $\mathbf{4}^{2+}$ on a glassy carbon electrode in 0.1 M Bu_4NClO_4/MeCN. Scan rate: 100 mV s^{-1}.

The anodic scan of asymmetric bis-ruthenium complex $\mathbf{2}^{3+}$ shows two chemically reversible oxidation waves at +0.61 and +1.58 V and an irreversible wave at +1.15 V versus Ag/AgCl. The redox couple at +0.61 V is due to oxidation of the cyclometalated ruthenium site (Ru2, Figure 1). This potential is in accordance with the oxidation potential of most reported cyclometalated monoruthenium complexes,[9] which also supports the formation of the Ru–C bond in complex $\mathbf{2}^{3+}$. The $Ru^{II/III}$ process that is associated with the $[Ru(bpy)_2]$ unit takes place at +1.58 V, which is more positive than the corresponding process in monoruthenium complex $\mathbf{1}^{2+}$. This result reflects the electron-withdrawing nature of the added ruthenium ion in complex $\mathbf{2}^{3+}$. The irreversible oxidation process at +1.15 V may be caused by ligand-based oxidative decomposition. Such a peak is commonly observed in cyclometalated ruthenium complexes.[9] Five cathodic waves are observed at −0.83, −1.29, −1.51, −1.73, and −1.88 V versus Ag/AgCl for complex $\mathbf{2}^{3+}$. The first two waves are assigned to the reduction of the bridging ligand and the other three waves are due to the reduction of the bpy and Mebip ligands. In comparison, the previously asymmetric bis-ruthenium complex $[(bpy)_2Ru(dpdpzH)Ru(tpy)](PF_6)_3$ (tpy = 2,2′,6′,2“-terpyridine) similarly showed three anodic waves and five cathodic waves.[14] However, the cyclometalated $Ru^{II/III}$ potential of complex $\mathbf{2}^{3+}$ is less positive, as a result of the electron-donating nature of the Mebip ligand.[19]

RuPt complex $\mathbf{4}^{2+}$ shows some ill-defined anodic waves (Figure 2c). However, the $Ru^{II/III}$ process appears at +1.57 V versus Ag/AgCl. Prior to the $Ru^{II/III}$ process, the irreversible waves may be due to oxidation of the platinum center or to the platinum-acetylide component.[10,15] Five cathodic redox couples can be observed within the solvent window of complex $\mathbf{4}^{2+}$ (−0.66, −1.20, −1.46, −1.67, and −2.00 V). The former two waves are attributable to the consecutive reductions of dpppz and the following two waves are assigned to the reductions of the bpy ligands. The origin of the fifth wave is unclear at this stage. These electrochemical behaviors are quite similar to the previously reported complex $[(bpy)_2Ru(dpdpzH)PtC{\equiv}CPh]^{2+}$.[15]

Table 1. Electrochemical data.[a]

Complex	$E_{1/2}$ (anodic)	$E_{1/2}$ (cathodic)
$\mathbf{1}^{2+}$, $[(bpy)_2Ru(dpppzH)](PF_6)_2$	+1.41	−0.96, −1.43, −1.64, −1.98
$\mathbf{2}^{3+}$, $[(bpy)_2Ru(dpppz)Ru(Mebip)](PF_6)_3$	+0.61, +1.15,[b] +1.58	−0.83, −1.29, −1.51, −1.73, −1.88
$\mathbf{4}^{2+}$, $[(bpy)_2Ru(dpppz)PtCCPh](PF_6)_2$	+1.35,[b] +1.57	−0.66, −1.20, −1.46, −1.67, −2.00
$[(bpy)_2Ru(dpp)](PF_6)_2$[c]	+1.38	−1.01, −1.49, −1.72
$[(bpy)_2Ru(dpdpzH_2)](PF_6)_2$[c]	+1.38	−0.97, −1.40, −1.73
$[(bpy)_2Ru(dpdpzH)Ru(tpy)](PF_6)_3$[c]	+0.81, +1.32,[b] +1.57	−0.82, −1.25, −1.55, −1.73, −1.90
$[(bpy)_2Ru(dpdpzH)PtCCPh](PF_6)_2$[c]	+1.37,[b] +1.58	−0.65, −1.23, −1.51, −1.79

[a] All measurements were performed in 0.1 M nBu_4NClO_4/MeCN. Unless otherwise stated, the potential is reported as $E_{1/2}$ versus Ag/AgCl. Potentials versus Fc/Fc$^+$ can be estimated by substracting 0.45 V. [b] Irreversible, $E_{peak,anodic}$. [c] See Ref. [14].

DFT Calculations

To assist in the understanding of the electronic structures of these complexes, DFT calculations have been performed on complexes $\mathbf{2}^{3+}$ and $\mathbf{4}^{2+}$ by using the B3LYP/LANL2DZ/6-31G*/CPCM method (for details, see the Experimental Section). The single-crystal structure of complex $\mathbf{2}^{3+}$ was used to generate the input file for the geometrical optimizations. The optimized bond lengths that are associated with the Ru1 and Ru2 atoms are slightly longer than those in the single-crystal structure (see the Supporting Information, Table S1). The Ru2–N8 bond (2.263 Å) is the longest of all of the calculated Ru–N bonds; the Ru2–N7, Ru2–N10, and Ru2–C1 bonds are relatively shorter (2.033, 2.032, and 2.036 Å, respectively). This trend is in agreement with the crystallographic data. The structure of complex $\mathbf{4}^{2+}$ was constructed on the basis of the DFT-optimized structure of complex $\mathbf{2}^{3+}$ by replacing the [Ru(Mebip)] component with [Pt–C≡CPh]. Table S2 in the Supporting Information shows selected bond lengths and angles in the DFT-optimized structure of complex **4**$^{2+}$. The Pt–C1 and Pt–C2 bond lengths are calculated to be 2.002 and 1.966 Å, respectively. The C1-Pt-N8 angle is 158.29°. These data agree well with those of known cyclometalated platinum complexes.[10]

Figure 3 and Figure 4 show the isodensity plots of the frontier orbitals for complexes **2**$^{3+}$ and **4**$^{2+}$, along with their corresponding energy diagrams, respectively. The HOMO, HOMO−1, and HOMO−2 of complex **2**$^{3+}$ are mainly associated with the cyclometalated ruthenium (Ru2) component. However, there is also significant electron density on the cyclometalating phenyl ring in the HOMO, a feature that is commonly present in cyclometalated complexes.[9,11] The lower-lying HOMO−3 and HOMO−4 levels have major contributions from the noncyclometalated ruthenium (Ru1) component. The LUMO and LUMO+1 are associated with the bridging ligand. The bpy ligands are responsible for the higher-lying LUMO+2 and LUMO+3 levels. The Mebip ligand makes a dominant contribution to the LUMO+4 and LUMO+5 levels. This order of orbital alignment suggests that the cyclometalated ruthenium atom in complex **2**$^{3+}$ is very likely to be oxidized prior to the noncyclometalated atom. Moreover, the DFT-optimized structure of the one-electron-oxidized form (**2**$^{4+}$) indicates a spin density that is dominated by the cyclometalated ruthenium component (see the Supporting Information, Figure S1). The order of reduction of complex **2**$^{3+}$ may take place from the bridging ligand, followed by the bpy and Mebip ligands. These results are consistent with the above assignments of the electrochemical behavior of complex **2**$^{3+}$.

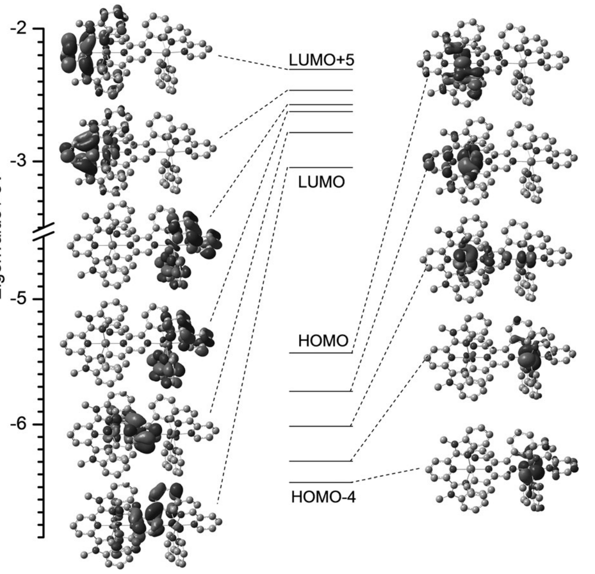

Figure 3. Isodensity plots of the frontier molecular orbitals of complex **2**$^{3+}$, along with the energy diagram.

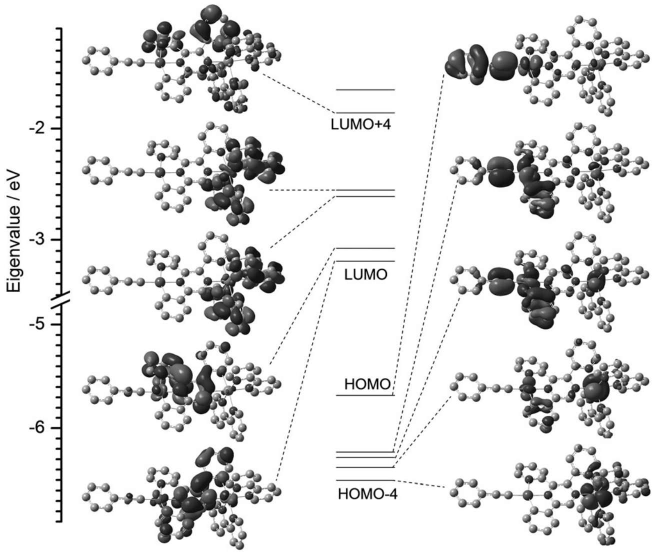

Figure 4. Isodensity plots of the frontier molecular orbitals of complex **4**$^{2+}$, along with the energy diagram.

The HOMO of complex **4**$^{2+}$ contains mixed contributions from the phenylacetylide component and the platinum atom (Figure 4). The HOMO−1 and HOMO−2 levels contain mixed contributions from the triple bond, the platinum atom, and the cyclometalating phenyl ring. The lower-lying HOMO−3 and HOMO−4 levels are dominated by the ruthenium component. The orbital compositions of the unoccupied orbitals in complex **4**$^{2+}$ share some similarities with those in complex **2**$^{3+}$. The LUMO and LUMO+1 levels are associated with the bridging ligand. The LUMO+2 and LUMO+3 levels are associated with the bpy ligands. The pyridine rings of the bridging ligand are responsible for the LUMO+4 orbital. Again, these results are consistent with the electrochemical behavior of complex **4**$^{2+}$, as shown in Figure 2.

Absorption Studies and TDDFT Calculations

The electronic absorption spectra of complexes **1**$^{2+}$, **2**$^{3+}$, and **4**$^{2+}$ are shown in Figure 5, along with those of previously reported complexes $[(bpy)_2Ru(dpdpzH_2)]^{2+}$ and $[(bpy)_2Ru(dpdpzH)PtC{\equiv}CPh]^{2+}$ for comparison.[14,15] The spectroscopic data are delineated in Table 2. In addition, TDDFT calculations have been performed on the above DFT-optimized structures of complexes **2**$^{3+}$ and **4**$^{2+}$ at the same level of theory and the predicted low-energy excitations are summarized in Table 3. Absorptions in the ultraviolet-light region are due to intraligand π–π* excitations. The metal-to-ligand charge-transfer (MLCT) transitions in complex **1**$^{2+}$ ($\lambda_{max}=427$ and 481 nm) are slightly blue-shifted relative to those in $[(bpy)_2Ru(dpdpzH_2)]^{2+}$ ($\lambda_{max}=446$ and 490 nm). Complex **2**$^{3+}$ showed an intense absorption band at 577 nm ($\varepsilon=0.41\times10^5\,\text{M}^{-1}\text{cm}^{-1}$). In addition, in the region 700–1000 nm, some weak-but-distinct absorption are present. TDDFT results suggest that the NIR absorption of complex **2**$^{3+}$ is associated with HOMO→LUMO+1 and HOMO→LUMO excitations (the S_1 and S_2 states, S stands for singlet). The S_{11} state, with an oscillator strength (f) of 0.3817, is likely responsible for the observed absorption band at

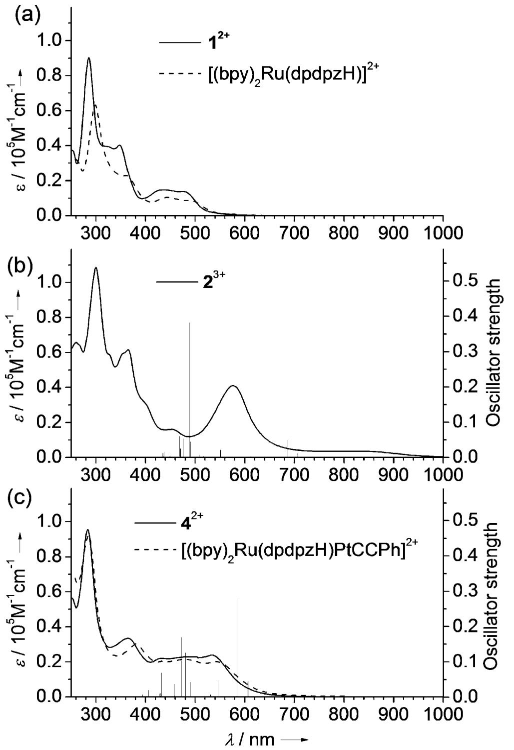

Figure 5. Electronic absorption spectra in MeCN and TDDFT results for a) 1^{2+}, b) 2^{3+}, and c) 4^{2+}. The right axes in (b) and (c) are associated with the TDDFT excitations for complexes 2^{3+} and 4^{2+}.

577 nm, although the predicted excitation is at higher energy. This state is mainly associated with the HOMO−2→LUMO+1 excitation (MLCT transition from the Ru2 atom to the bridging ligand) and has minor contributions from the HOMO−1→LUMO+4, HOMO→LUMO+3, and HOMO→LUMO+5 excitations (MLCT transition from the Ru2 atom to the Mebip or bpy ligands). Inconsistency between the TDDFT-predicted excitation energy and the experimental value is often observed in charge-transfer transitions in metal complexes. The weaker absorption band of complex $\mathbf{2}^{3+}$ at 456 nm is assigned to MLCT transitions from the noncyclometalated ruthenium (Ru1) component.

RuPt complex $\mathbf{4}^{2+}$ has a very similar absorption spectrum to $[(bpy)_2Ru(dpdpzH)PtC{\equiv}CPh]^{2+}$, with a slightly blue-shifted low-energy absorption edge. The TDDFT results suggest that the absorption band of complex $\mathbf{4}^{2+}$, with $\lambda_{max} = 534$ nm, contains a major component from the HOMO→LUMO+1 excitation (the S_2 state), which can be interpreted as a mixture of platinum-based MLCT transitions and ligand-to-ligand charge-transfer (LLCT) from the phenyl-acetylide unit. The ruthenium-based MLCT transitions are very likely within the region 400–500 nm. A similar situation has previously been observed for $[(bpy)_2Ru(dpdpzH)PtC{\equiv}CPh]^{2+}$.[15]

Emission Studies

The previously reported monoruthenium complex $[(bpy)_2Ru(dpdpzH_2)]^{2+}$ exhibited an emission band at 709 nm and $\phi = 0.057\,\%$ (Table 2 and Figure 6).[14] The excited-state lifetime (τ) of this complex was later determined to be 41 ns under ambient conditions in dilute MeCN. The newly prepared ruthenium complex $\mathbf{1}^{2+}$, which contains the dpppz ligand, shows an emission band at 695 nm. This slightly blue-shifted emission maximum relative to complex $[(bpy)_2Ru(dpdpzH_2)]^{2+}$ is in accordance with the difference in their absorption spectra. To our delight, complex $\mathbf{1}^{2+}$ displays a much higher ϕ value (2.9 %) and a longer lifetime (302 ns) under the same experimental conditions. These results suggest that the free-standing phenyl rings in the dpdpz ligand provide a non-emissive deactivation pathway, as discussed in the design strategy of dpppzH (see the Introduction).

Table 2. Absorption and emission data.[a]

Complex	Absorption λ_{max} [nm] (ε [$\times10^5$ $M^{-1}cm^{-1}$])	Emission[b] λ_{max} [nm]/ϕ [%]/τ [ns]
$\mathbf{1}^{2+}$, $[(bpy)_2Ru(dpppzH)](PF_6)_2$	285 (0.90), 347 (0.40), 427 (0.15), 481 (0.14)	695/2.9/302
$\mathbf{2}^{3+}$, $[(bpy)_2Ru(dpppz)Ru(Mebip)](PF_6)_3$	299 (1.08), 365 (0.61), 456 (0.16), 577 (0.41), 834 (0.04)	no emission detected
$\mathbf{4}^{2+}$, $[(bpy)_2Ru(dpppz)PtCCPh](PF_6)_2$	282 (0.95), 363 (0.33), 426 (0.22), 468 (0.22), 534 (0.24)	752/0.41/170
$[(bpy)_2Ru(dpp)](PF_6)(PF_6)_2$[c]	430(0.12), 470(0.10)	675/5.1/135
$[(bpy)_2Ru(dpdpzH_2)](PF_6)_2$[d]	299 (0.63), 360 (0.23), 446 (0.10), 490 (0.088)	709/0.057/41
$[(bpy)_2Ru(dpdpzH)PtCCPh](PF_6)_2$[d]	286 (0.78), 380 (0.30), 436 (0.20), 477 (0.20), 545 (0.20)	780/0.15/120

[a] All spectra were recorded in MeCN at room temperature. [b] Excitation wavelength: 400 nm for all compounds studied. Quantum yield was determined by comparison with $[Ru(bpy)_3](PF_6)_2$, which had a quantum yield of 5.9 % in N_2-saturated MeCN. [c] See Ref. [6a]. [d] See Ref. [14].

No emission for bis-ruthenium complex $\mathbf{2}^{3+}$ was detected at room temperature. Possible emission from the $[Ru(bpy)_2]$

Table 3. TDDFT results.[a]

Complex	S_n	E [eV]	λ[nm]	f	Dominant transition(s) (percentage contribution[b])	Assignment[c]
2^{3+}	1	1.75	706.6	0.0105	HOMO→LUMO+1 (77)	$M_{Ru2}L_{BL}CT$
	2	1.81	686.8	0.0491	HOMO→LUMO (74)	$M_{Ru2}L_{BL}CT$
	6	2.25	550.8	0.0214	HOMO−2→LUMO (92)	$M_{Ru2}L_{BL}CT$
	10	2.53	490.5	0.0453	HOMO→LUMO+3 (76)	$M_{Ru2}L_{bpy}CT$
	11	2.54	488.8	0.3817	HOMO−2→LUMO+1 (44) HOMO−1→LUMO+4 (12) HOMO→LUMO+3 (11) HOMO→LUMO+5 (10)	$M_{Ru2}L_{BL}CT$ $M_{Ru2}L_{Mebip}CT$ $M_{Ru2}L_{bpy}CT$ $M_{Ru2}L_{Mebip}CT$
	12	2.60	476.0	0.0538	HOMO−2→LUMO+4 (83)	$M_{Ru2}L_{Mebip}CT$
	14	2.65	467.9	0.0604	HOMO−1→LUMO+5 (98)	$M_{Ru2}L_{Mebip}CT$
4^{2+}	1	2.04	606.5	0.0444	HOMO→LUMO (73)	$M_{Pt}L_{BL}CT$/LLCT
	2	2.12	584.4	0.2798	HOMO→LUMO+1 (72)	$M_{Pt}L_{BL}CT$/LLCT
	3	2.27	546.4	0.0478	HOMO−3→LUMO (46) HOMO−2→LUMO (24) HOMO−1→LUMO (18)	$M_{Ru}L_{BL}CT$ $M_{Pt}L_{BL}CT$ $M_{Pt}L_{BL}CT$
	7	2.53	289.7	0.0423	HOMO−1→LUMO+1 (35) HOMO−1→LUMO (29) HOMO−2→LUMO+1 (17) HOMO−2→LUMO (14)	$M_{Pt}L_{BL}CT$ $M_{Pt}L_{BL}CT$ $M_{Pt}L_{BL}CT$ $M_{Pt}L_{BL}CT$
	8	2.58	480.1	0.1258	HOMO−2→LUMO+1 (34) HOMO−3→LUMO+1 (23) HOMO−1→LUMO+1 (13)	$M_{Pt}L_{BL}CT$ $M_{Ru}L_{BL}CT$ $M_{Pt}L_{BL}CT$
	9	2.63	471.7	0.1698	HOMO−3→LUMO+1 (50)	$M_{Ru}L_{BL}CT$
	11	2.71	457.4	0.0373	HOMO−5→LUMO (52)	$M_{Ru}L_{BL}CT$
	15	2.87	432.1	0.0686	HOMO−5→LUMO+1 (60)	$M_{Ru}L_{BL}CT$

[a] Computed at the B3LYP/LANL2DZ/6-31G*/CPCM level of theory. [b] Actual contribution [%] = (configuration coefficient)^2 × 2 × 100. [c] BL = bridging ligand. The Ru2 atom in complex 2^{3+} is the cyclometalated one.

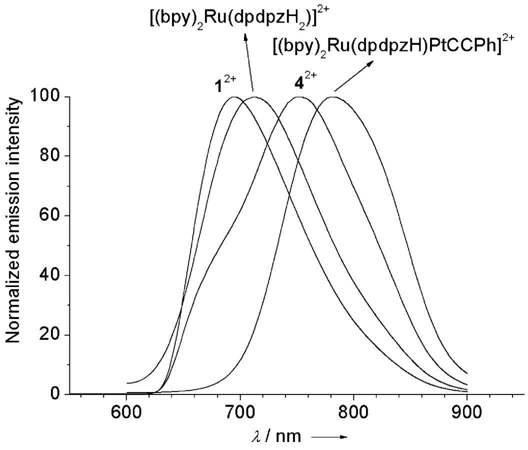

Figure 6. Normalized emission spectra in MeCN at room temperature. Excitation wavelength: 400 nm.

component could be quenched by the cyclometalated ruthenium moiety, as a result of an energy-transfer process. Similar cyclometalated ruthenium-induced energy transfer and emission quench have been reported previously.[14,23]

The previously reported heterobimetallic RuPt complex $[(bpy)_2Ru(dpdpzH)PtC{\equiv}CPh]^{2+}$ emits at 780 nm, with ϕ = 0.15 %.[15] The excited-state lifetime of $[(bpy)_2Ru(dpdpzH)PtC{\equiv}CPh]^{2+}$ was later determined to be 120 ns. The dpppz-bridged RuPt complex 4^{2+} shows an emission band at about 750 nm, with ϕ = 0.41 % and a lifetime of 170 ns. The emission maximum of compound 4^{2+} is slightly blue-shifted relative to that of $[(bpy)_2Ru(dpdpzH)PtC{\equiv}CPh]^{2+}$, in accordance with their absorption spectra, as shown in Figure 5. It has been reported that the excited-state lifetime of bis-tridentate ruthenium complexes can be prolonged by forming a two-metal system, which stabilizes the ligand π*-acceptor orbital and lowers the MLCT state below the deactivating ligand-field state.[24] However, previous TDDFT results have shown that the lowest MLCT transitions are mainly associated with the platinum-acetylide component. Thus, we believe that the NIR emission of complex 4^{2+} is a Pt-based MLCT/LLCT, as a result of an energy-transfer process from the excited Ru-based MLCT state to the Pt-based charge-transfer level.[25] The enhanced ϕ value and prolonged lifetime of complex 4^{2+} with respect to $[(bpy)_2Ru(dpdpzH)PtC{\equiv}CPh]^{2+}$ are presumably a combined result of the energy-gap law and the absence of a free-standing phenyl ring in the bridging ligand in complex 4^{2+}.

Conclusions

In summary, a new NN-CNN-type bridging ligand 2,3-di(2-pyridyl)-5-phenylpyrazine has been developed for the synthesis of bimetallic complexes with interesting spectroscopic and electrochemical properties. The asymmetric nature of this ligand allows for the construction of heterobimetallic complexes or homobimetallic complexes with different coordination modes, as exemplified by RuPt complex 4^{2+} and bis-ruthenium complex 2^{3+}. As a result of the absence of free-rotating phenyl groups, these new complexes display enhanced emission quantum yields and prolonged excited-state lifetimes with respect to the previously reported Ru and RuPt complexes with 2,3-di(2-pyridyl)-5,6-phenylpyrazine. These properties make the RuPt complex potentially useful for the photocatalytic reduction of water.[26] The newly developed bridging ligand will also be useful for the construction of other bimetallic complexes with mixed non-cyclometalated and cyclometalated coordination modes.

Experimental Section

Synthesis

General

Solution NMR spectra were recorded on a Bruker Avance 400 MHz spectrometer. ^{1}H NMR spectra are reported in ppm and are referenced to residual protons in the deuterated solvent ($\delta = 7.26$ ppm for $CDCl_3$ and $\delta = 1.92$ ppm for CD_3CN). MS data were obtained on Bruker Daltonics Inc. Apex II FT-ICR or Autoflex III MALDI-TOF mass spectrometers. The matrix for the matrix-assisted laser desorption ionization time-of-flight (MALDI-TOF) measurements is α-cyano-4-hydroxycinnamic acid. Microanalysis was performed on Flash EA 1112 or Carlo Erba 1106 analyzers at the Institute of Chemistry, the Chinese Academy of Sciences. Ferroceneboronic acid was purchased from Aladdin reagent of China.

Synthesis of 2,3-Di(2-pyridyl)-5-phenylpyrazine (dpppzH)

A solution of 2,2′-pyridil (1.70 g, 8.0 mmol) and 1-phenylethylenediamine (1.10 g, 8.0 mmol) in EtOH (40 mL) was heated at reflux for 20 h under a nitrogen atmosphere. After cooling to RT, the mixture was opened to air and stirred for a further 3 days. The resulting yellow precipitate was collected and purified by flash column chromatography on silica gel (CH_2Cl_2/EtOAc/NH_4OH, 20:80:0.2) to give dpppzH as a yellow solid (1.55 g, 63 % yield). ^{1}H NMR (400 MHz, $CDCl_3$): $\delta = 7.23$ (m, 2 H), 7.50–7.54 (m, 3 H), 7.76–7.84 (m, 3 H), 8.02 (d, $J = 7.8$ Hz, 1 H), 8.17 (d, $J = 7.0$ Hz, 2 H), 8.38 (dd, $J = 15.0$, 4.8 Hz, 2 H), 9.11 ppm (s, 1 H); ^{13}C NMR (100 MHz, $CDCl_3$): $\delta = 122.79$, 123.08, 124.13, 124.32, 127.19, 129.05, 130.04, 135.99, 136.44, 136.61, 139.52, 148.51, 148.77, 150.23, 150.34, 151.32, 157.06, 157.29 ppm; MS (EI): m/z: 309 $[M-H]^+$, HRMS (EI): m/z calcd for $C_{20}H_{13}N_4$: 309.1139 $[M-H]^+$; found: 309.1144.

Synthesis of $[(bpy)_2Ru(dpppzH)](PF_6)_2$ ($\mathbf{1}^{2+}$)

To a solution of dpppzH (62 mg, 0.20 mmol) in ethylene glycol (10 mL) was added *cis*-$[Ru(bpy)_2Cl_2]\cdot 2H_2O$ (104 mg, 0.20 mmol) and the mixture was heated under microwave irradiation for 30 min (375 W). After cooling to RT, excess KPF_6 (aq) was added. The resulting precipitate was collected and purified by flash column chromatography on silica gel (MeCN/H_2O/aq. KNO_3, 150:10:1) to give complex $\mathbf{1}^{2+}$ as a red solid (140 mg, 64 % yield). ^{1}H NMR (400 MHz, CD_3CN): $\delta = 7.22$ (d, $J = 8.3$ Hz, 1 H), 7.28 (t, $J = 6.2$ Hz, 1 H), 7.43–7.53 (m, 7 H), 7.65–7.67 (m, 2 H), 7.69 (d, $J = 5.5$ Hz, 1 H), 7.73 (d, $J = 5.4$ Hz, 1 H), 7.78–7.83 (m, 4 H), 8.06–8.15 (m, 8 H), 8.51 (d, $J = 7.2$ Hz, 2 H), 8.53 (d, $J = 8$ Hz, 2 H), 8.65 ppm (d, $J = 4.6$ Hz, 1 H); ^{13}C NMR (100 MHz, CD_3CN): $\delta = 125.77$, 125.82, 125.99, 126.23, 127.10, 128.50, 128.79, 128.82, 129.06, 129.16, 129.22, 130.56, 132.92, 135.04, 137.99, 139.57, 139.59, 139.67, 139.73, 139.76, 142.45, 151.10, 151.23, 152.77, 152.87, 152.99, 153.40, 153.50, 153.66, 155.46, 156.84, 157.60, 157.86, 158.11, 158.27, 158.31 ppm; MS (MALDI): m/z: 869.0 $[M-PF_6]^+$, 724.1 $[M-2PF_6]^+$; elemental analysis calcd [%] for $C_{40}H_{30}F_{12}N_8P_2Ru_2\cdot H_2O$: C 46.57, H 3.11, N 10.86; found: C 46.22, H 3.23, N 10.78.

Synthesis of $[(bpy)_2Ru(dpppz)Ru(Mebip)](PF_6)_3$ ($\mathbf{2}^{3+}$)

To a solution of $[(Mebip)RuCl_3]$[19] (27.0 mg, 0.050 mmol) in dry acetone (15 mL) was added AgOTf (78.0 mg, 0.30 mmol) and the mixture was heated at reflux for 2 h under a nitrogen atmosphere. After cooling to RT, the generated AgCl precipitate was removed by filtering through a pad of Celite. The filtrate was concentrated under reduced pressure. The above-prepared monoruthenium complex $\mathbf{1}^{2+}$ (51.0 mg, 0.050 mmol), DMF (10 mL), and *t*BuOH (10 mL) were added to the residue. The resulting mixture was heated at reflux under a nitrogen atmosphere for a further 24 h. The solvent was removed under reduced pressure. The residue was dissolved in MeOH (1 mL), followed by the addition of excess aqueous KPF_6. The resulting precipitate was collected and purified by flash column chromatography on silica gel (MeCN/H_2O/aq. KNO_3, 150:10:3), followed by anion exchange with KPF_6, to give complex $\mathbf{2}^{3+}$ as a deep purple solid (20.0 mg, 25 % yield). MS (MALDI): m/z: 1307.2 $[M-2PF_6-H]^+$, 1163.2 $[M-3PF_6]^+$, 1005.1 $[M-3PF_6-bpy]^+$; elemental analysis calcd [%] for $C_{61}H_{46}F_{18}N_{13}P_3Ru_2\cdot 3H_2O$: C 44.34, H 3.17, N 11.02; found: C 44.28, H 3.03, N 11.32.

Synthesis of $[(bpy)_2Ru(dpppz)PtCl](PF_6)_2$ ($\mathbf{3}^{2+}$)

An aqueous solution of K_2PtCl_4 (15 mL, 0.20 mmol, 82.0 mg) was added to a solution of monoruthenium complex $\mathbf{1}^{2+}$ (0.10 mmol, 102 mg) in MeCN (15 mL). The mixture was heated at reflux for 24 h under a nitrogen atmosphere. After cooling to RT, the organic solvent was evaporated before adding an excess of aqueous KPF_6. The resulting precipitate was collected to afford complex $\mathbf{3}^{2+}$ as a deep red solid (112 mg, 90 % yield). This crude product was used in the next transformation without further purification. MS (MALDI): m/z: 952.7 $[M-2PF_6]^+$.

Synthesis of $[(bpy)_2Ru(dpppz)PtC{\equiv}CPh](PF_6)_2$ ($\mathbf{4}^{2+}$)

The above-prepared complex $\mathbf{3}^{2+}$ (50.0 mg, 0.040 mmol), CuI (2.0 mg), and phenylacetylene (0.30 mL, 0.30 mmol) were added to a mixture of nitrogen-saturated DMF (10 mL) and triethylamine (2 mL). The mixture was stirred in the dark at RT for 22 h. The solvent was removed under reduced pressure. The residue was purified by flash column chromatography on silica gel (MeCN/H_2O/aq. KNO_3, 200:10:1), followed by anion exchange with an aqueous solution of KPF_6, to give complex $\mathbf{4}^{2+}$ as a deep-brown solid (36 mg, 70 % yield). MS (MALDI): m/z: 1161.6 $[M-PF_6]^+$, 1017.7 $[M-2PF_6]^+$, 861.8 $[M-2PF_6-bpy]^+$; elemental analysis calcd [%] for $C_{48}H_{34}F_{12}N_8P_2PtRu\cdot H_2O$: C 43.45, H 2.73, N 8.44; found: C 43.52, H 2.77, N 8.83.

Spectroscopic Measurements

Absorption spectra were obtained on a TU-1810DSPC spectrometer (Beijing Purkinje General Instrument Co. Ltd.) at RT in MeCN in a conventional quartz cell (path length: 1 cm). Emission spectra were recorded on a F-380 spectrofluorimeter (Tianjin Gangdong Sic. & Tech Development Co. Ltd.), with a red-light-sensitive R928F photomultiplier tube. Samples for the emission measurements were placed in quartz cuvettes (path length: 1 cm). Luminescence quantum yields were determined by using $[Ru(bpy)_3](PF_6)_2$ in degassed MeCN as a standard ($\phi = 5.9\,\%$).[27] The excited-state lifetime was determined on a Hamamatsu Quantaurus-Tau under ambient conditions at RT.

X-ray Crystallography

X-ray diffraction data were collected on a Rigaku Saturn 724 diffractometer with a rotating anode ($Mo_{K\alpha}$ radiation, 0.71073 Å) at 173 K. The structure was solved by using direct methods with SHELXS-97[28] and refined with Olex2.[29] The structure shown in Figure 1 was generated by using Olex2.

Electrochemical Measurements

All cyclic voltammetry (CV) measurements were recorded on a CHI620D potentiostat with a one-compartment electrochemical cell under a nitrogen atmosphere. All of the measurements were recorded in 0.1 M Bu_4NClO_4 in indicated solvents at a scan rate of 100 mV s^{-1}. The working electrode was a glassy carbon electrode with a diameter of 0.3 mm. The electrode was polished prior to use with 0.05 μm alumina and thoroughly rinsed with water and acetone. A large-area platinum wire coil was used as the counter electrode. All potentials are referenced to a Ag/AgCl electrode in a saturated aqueous solution of NaCl without regard for the liquid-junction potential.

Computational Methods

All calculations were implemented in the Gaussian 09 program.[30] Wavefunctions were expanded in the LANL2DZ basis set with effective core potentials[31] and the electron-exchange correlation was described by using the B3LYP hybrid functional.[32] Solvation effects in MeCN were included by using the conductor-like polarizable continuum model (CPCM) with united-atom Kohn–Sham (UAKS) radii.[33] All orbitals were computed at an isovalue of 0.03 *e* bohr^{-3}.

Acknowledgements

This work was supported by the National Natural Science Foundation of China (91227104, 21002104, 212210017, and 21271176), the National Basic Research 973 Program of China (2011CB932301), the Scientific Research Foundation for Returned Overseas Chinese Scholars, the State Education Ministry of China, and the Institute of Chemistry at the Chinese Academy of Sciences (100 Talent Program, CMS-PY-201230).

---

[1] a) J.-P. Sauvage, J.-P. Collin, J.-C. Chambron, S. Gullerez, C. Coudret, *Chem. Rev.* **1994**, *94*, 993; b) U. S. Schubert, C. Eschbaumer, *Angew. Chem.* **2002**, *114*, 3016; *Angew. Chem. Int. Ed.* **2002**, *41*, 2892; c) J.-P. Collin, P. Laine, J.-P. Launay, J.-P. Sauvage, A. Sour, *J. Chem. Soc. Chem. Commun.* **1993**, 434; d) J. Bolger, A. Gourdon, E. Ishow, J.-P. Launay, *J. Chem. Soc. Chem. Commun.* **1995**, 1799; e) P. Bonhote, A. Lecas, E. Amouyal, *Chem. Commun.* **1998**, 885; f) A. Gourdon, J.-P. Launay, *Inorg. Chem.* **1998**, *37*, 5336; g) E. Ishow, A. Gourdon, J.-P. Launay, C. Chiorboli, F. Scandola, *Inorg. Chem.* **1999**, *38*, 1504; h) A. L. Sauers, D. M. Ho, S. Bernhard, *J. Org. Chem.* **2004**, *69*, 8910; i) C. N. Carlson, C. J. Kuehl, R. E. Da Re, J. M. Veauthier, E. J. Schelter, A. E. Milligan, B. L. Scott, E. D. Bauer, J. D. Thompson, D. E. Morris, K. D. John, *J. Am. Chem. Soc.* **2006**, *128*, 7230; j) D. M. D'Alessandro, P. H. Dinolfo, M. S. Davis, J. T. Hupp, F. R. Keene, *Inorg. Chem.* **2006**, *45*, 3261; k) S. Singh, N. R. de Tacconi, N. R. G. Diaz, R. O. Lezna, J. M. Zuniga, K. Abayan, F. M. MacDonnell, *Inorg. Chem.* **2011**, *50*, 9318.

[2] a) B. Ulgut, H. D. Abruña, *Chem. Rev.* **2008**, *108*, 2721; b) P. J. Low, *Dalton Trans.* **2005**, 2821; c) M. Akita, T. Koike, *Dalton Trans.* **2008**, 3523; d) N. Tuccitto, V. Ferri, M. Cavazzini, S. Quici, G. Zhavnerko, A. Licciardello, M. A. Rampi, *Nat. Mater.* **2009**, *8*, 41; e) J.-W. Ying, I. P.-C. Liu, B. Xi, Y. Song, C. Campana, J.-L. Zuo, T. Ren, *Angew. Chem.* **2010**, *122*, 966; *Angew. Chem. Int. Ed.* **2010**, *49*, 954.

[3] a) R. M. Leasure, W. Ou, J. A. Moss, R. W. Linton, T. J. Meyer, *Chem. Mater.* **1996**, *8*, 264; b) S. Bernhard, J. I. Goldsmith, K. Takada, H. D. Abruña, *Inorg. Chem.* **2003**, *42*, 4389; c) C.-J. Yao, Y.-W. Zhong, H.-J. Nie, H. D. Abruña, J. Yao, *J. Am. Chem. Soc.* **2011**, *133*, 20720; d) C.-J. Yao, J. Yao, Y.-W. Zhong, *Inorg. Chem.* **2012**, *51*, 6259.

[4] a) W.-Y. Wong, C.-L. Ho, *Acc. Chem. Res.* **2010**, *43*, 1246; b) S. Diring, R. Ziessel, F. Barigelletti, A. Barbieri, B. Ventura, *Chem. Eur. J.* **2010**, *16*, 9226; c) S. Goeb, A. De Nicola, R. Ziessel, C. Sabatini, A. Barbieri, F. Barigelletti, *Inorg. Chem.* **2006**, *45*, 1173; d) A. C. Benniston, A. Harriman, P. Li, C. A. Sams, *J. Am. Chem. Soc.* **2005**, *127*, 2553.

[5] a) C. R. Arana, H. D. Abruña, *Inorg. Chem.* **1993**, *32*, 194; b) L. M. Vogler, B. Scott, K. J. Brewer, *Inorg. Chem.* **1993**, *32*, 898; c) R. Ruminski, J. Kiplinger, T. Cockroft, C. Chase, *Inorg. Chem.* **1989**, *28*, 370; d) L. M. Vogler, K. J. Brewer, *Inorg. Chem.* **1996**, *35*, 818; e) C. M. Hartshorn, N. Daire, V. Tondreau, B. Loeb, T. J. Meyer, P. S. White, *Inorg. Chem.* **1999**, *38*, 3200; f) D. M. Dattelbaum, C. M. Hartshom, T. J. Meyer, *J. Am. Chem. Soc.* **2002**, *124*, 4938; g) N. Chanda, B. Sarkar, S. Kar, J. Fiedler, W. Kaim, G. K. Lahiri, *Inorg. Chem.* **2004**, *43*, 5128; h) S. Flores-Torres, G. R. Hutchison, L. J. Stoltzberg, H. D. Abruña, *J. Am. Chem. Soc.* **2006**, *128*, 1513.

[6] a) C. H. Braunstein, A. D. Baker, T. C. Strekas, H. D. Gafney, *Inorg. Chem.* **1984**, *23*, 857; b) R. Sahai, L. Morgan, D. P. Rillema, *Inorg. Chem.* **1988**, *27*, 3495; c) G. Denti, S. Campagna, L. Sabatino, S. Serroni, M. Ciano, V. Balzani, *Inorg. Chem.* **1990**, *29*, 4750; d) S. Serroni, G. Denti, S. Campagna, A. Juris, M. Ciano, V. Balzani, *Angew. Chem.* **1992**, *104*, 1540; *Angew. Chem. Int. Ed. Engl.* **1992**, *31*, 1493; e) M. M. Richter, K. J. Brewer, B. J. Yoblinski, M. Stathis, T. F. Guarr, *Inorg. Chem.* **1992**, *31*, 1594; f) M. M. Richter, K. J. Brewer, *Inorg. Chem.* **1993**, *32*, 2827; g) S. Serroni, A. Juris, S. Campagna, M. Venturi, G. Denti, V. Balzani, *J. Am. Chem. Soc.* **1994**, *116*, 9086; h) V. Balzani, S. Campagna, G. Denti, A. Juris, S. Serroni, M. Venturi, *Acc. Chem. Res.* **1998**, *31*, 26; i) M. Marcaccio, F. Paolucci, C. Paradisi, S. Roffia, C. Fontanesi, L. J. Yellowlees, S. Serroni, S, Campagna, G. Denti, V. Balzani, *J. Am. Chem. Soc.* **1999**, *121*, 10081.

[7] a) M. I. Bruce, *Angew. Chem.* **1977**, *89*, 75; *Angew. Chem. Int. Ed. Engl.* **1977**, *16*, 73; b) M. E. van der Boom, D. Milstein, *Chem. Rev.* **2003**, *103*, 1759; c) Y. Chi, P.-T. Chou, *Chem. Soc. Rev.* **2010**, *39*, 638; d) G. van Koten, D. Milstein, *Organometallic Pincer Chemistry, Topics in Organometallic Chemistry, Vol. 40*, Springer, Heidelberg, **2013**.

[8] a) Y. You, S. Y. Park, *Dalton Trans.* **2009**, 1267; b) Z.-q. Chen, Z.-q. Bian, C.-H. Huang, *Adv. Mater.* **2010**, *22*, 1534; c) M. Polson, M. Ravaglia, S. Fracasso, M. Garavelli, F. Scandola, *Inorg. Chem.* **2005**, *44*, 1282; d) A. J. Wilkinson, A. E. Goeta, C. Foster, J. A. G. Williams, *Inorg. Chem.* **2004**, *43*, 6513; e) Y.-C. Zhu, L. Zhou, H.-Y. Li, Q.-L. Xu, M.-Y. Teng, Y.-X. Zheng, J.-L. Zuo, H.-J. Zhang, X.-Z. You, *Adv. Mater.* **2011**, *23*, 4041.

[9] a) C. Coudret, S. Fraysse, J.-P. Launay, *Chem. Commun.* **1998**, 663; b) S. H. Wadman, J. M. Kroom, K. Bakker, M. Lutz, A. L. Spek, G. P. M. van Klink, G. van Koten, *Chem. Commun.* **2007**, 1907; c) J.-P. Djukic, J.-B. Sortais, L. Barloy, M. Pfeffer, *Eur. J. Inorg. Chem.* **2009**, 817; d) B. D. Koivisto, K. C. D. Robson, C. P. Berlinguette, *Inorg. Chem.* **2009**, *48*, 9644; e) M. Jäger, A. Smeigh, F. Lombeck, H. Görls, J.-P. Collin, J.-P. Sauvage, L. Hammarström, O. Johannsson, *Inorg. Chem.* **2010**, *49*, 374; f) S. H. Wadman, J. M. Kroon, K. Bakker, R. W. A. Havenith, G. P. M. van Klink, G. van Koten, *Organometallics* **2010**, *29*, 1569; g) W.-W. Yang, L. Wang, Y.-W. Zhong, J. Yao, *Organometallics* **2011**, *30*, 2236; h) C.-J. Yao, R.-H. Zheng, Q. Shi, Y.-W. Zhong, J. Yao, *Chem. Commun.* **2012**, *48*, 5680.

[10] a) W. Lu, B.-X. Mi, M. C. W. Chan, Z. Hui, C.-M. Che, N. Zhu, S.-T. Lee, *J. Am. Chem. Soc.* **2004**, *126*, 4958; b) P. Shao, Y. Li, J. Yi, T. M. Pritchett, W. Sun, *Inorg. Chem.* **2010**, *49*, 4507; c) A. Hofmann, L. Dahlenburg, R. van Eldik, *Inorg. Chem.* **2003**, *42*, 6528; d) T.-C. Cheung, K.-K. Cheung, S.-M. Peng, C.-M. Che, *J. Chem. Soc. Dalton Trans.* **1996**, 1645; e) J. Ni, X. Zhang, Y.-H. Wu, L.-Y. Zhang, Z.-N. Chen, *Chem. Eur. J.* **2011**, *17*, 1171.

[11] a) C.-J. Yao, Y.-W. Zhong, J. Yao, *J. Am. Chem. Soc.* **2011**, *133*, 15697; b) L.-Z. Sui, W.-W. Yang, C.-J. Yao, H.-Y. Xie, Y.-W. Zhong, *Inorg. Chem.* **2012**, *51*, 1590.

[12] C.-J. Yao, L.-Z. Sui, H.-Y. Xie, W.-J. Xiao, Y.-W. Zhong, J. Yao, *Inorg. Chem.* **2010**, *49*, 8347.

[13] a) M. Beley, J.-P. Collin, R. Louis, B. Metz, J.-P. Sauvage, *J. Am. Chem. Soc.* **1991**, *113*, 8521; b) J.-P. Sutter, D. M. Grove, M. Beley, J.-P. Collin, N. Veldman, A. L. Spek, J.-P. Sauvage, G. van Koten, *Angew. Chem.* **1994**, *106*, 1359; *Angew. Chem. Int. Ed. Engl.* **1994**, *33*, 1282; c) C. Patoux, J.-P. Launay, M. Beley, S. Chodorowski-Kimmers, J.-P. Collin, S. James, J.-P. Sauvage, *J. Am. Chem. Soc.* **1998**, *120*, 3717; d) P. Steenwinkel, D. M. Grove, N. Veldman, A. L. Spek, G. van Koten, *Organometallics* **1998**, *17*, 5647; e) S. Fraysse, C. Coudret, J.-P. Launay, *J. Am. Chem. Soc.* **2003**, *125*, 5880; f) M. Gagliardo, C. H. M. Amijs, M. Lutz, A. L. Spek, R. W. A. Havenith, F. Hartl, G. P. M. van Klink, G. van Koten, *Inorg. Chem.* **2007**, *46*, 11133.

[14] a) Y.-W. Zhong, S.-H. Wu, S. E. Burkhardt, C.-J. Yao, H. D. Abruña, *Inorg. Chem.* **2011**, *50*, 517; b) S.-H. Wu, S. E. Burkhardt, Y.-W. Zhong, H. D. Abruña, *Inorg. Chem.* **2012**, *51*, 13312.

[15] S.-H. Wu, S. E. Burkhardt, J. Yao, Y.-W. Zhong, H. D. Abruña, *Inorg. Chem.* **2011**, *50*, 3959.

[16] S.-H. Wu, H. D. Abruña, Y.-W. Zhong, *Organometallics* **2012**, *31*, 1161.

[17] a) J. Fabian, H. Makazumi, M. Matsuoka, *Chem. Rev.* **1992**, *92*, 1197; b) G. Qian, Z. Y. Wang, *Chem. Asian J.* **2010**, *5*, 1006.

[18] a) S. Shatzmiller, S. Bercovici, *Liebigs Ann. Chem.* **1992**, 1005; b) L. M. Hryhorczuk, J. C. Bailar, Jr., *Inorg. Chem.* **1985**, *24*, 3367; c) L. Maier, P. J. Diel, *Phosphorous Sulfur Silicon Relat. Elem.* **1995**, *107*, 245.

[19] W.-W. Yang, Y.-W. Zhong, S. Yoshikawa, J.-Y. Shao, S. Masaoka, K. Sakai, J. Yao, M.-a. Haga, *Inorg. Chem.* **2012**, *51*, 890.

[20] a) S. L. James, M. Younus, P. R. Raithby, J. Lewis, *J. Organomet. Chem.* **1997**, *543*, 233; b) M. Hissler, J. E. McGarrah, W. B. Connick, D. K. Geiger, S. D. Cummings, R. Eisenberg, *Coord. Chem. Rev.*

2000, *208*, 115; c) M. Hissler, W. B. Connick, D. K. Geiger, J. E. McGarrah, D. Lipa, R. J. Lachicotte, R. Eisenberg, *Inorg. Chem.* **2000**, *39*, 447; d) V. W.-W. Yam, K. H.-Y. Chan, K. M.-C. Wong, B. W.-K. Chu, *Angew. Chem.* **2006**, *118*, 6315; *Angew. Chem. Int. Ed.* **2006**, *45*, 6169; e) J. B. Seneclauze, P. Retailleau, R. Ziessel, *New J. Chem.* **2007**, *31*, 1412.

[21] Crystallographic data for [**2**](PF_6)$_3$: $C_{61}H_{46}F_{18}N_{13}P_3Ru_2$; M_w = 1598.16; monoclinic; space group $P21/c$; a = 11.673(3), b = 17.288(5), c = 38.114(11) Å; α = 90.00, β = 98.880(3), γ = 90.00°; U = 7599(4) Å^3; T = 173 K; Z = 4; 16004 reflections measured; $Mo_{K\alpha}$ radiation (λ = 0.71073 Å); final R indices R_1 = 0.0981, wR_2 = 0.2634; R indices (all data) R_1 = 0.1167, wR_2 = 0.2746. CCDC 936001 contains the supplementary crystallographic data for [**2**](PF_6)$_3$. This data can be obtained free of charge from the Cambridge Crystallographic Data Centre via www.ccdc.cam.ac.uk/data request/cif.

[22] a) P. Reveco, R. H. Schmehl, W. R. Cherry, F. R. Fronczek, J. Selbin, *Inorg. Chem.* **1985**, *24*, 4078; b) S. H. Wadman, M. Lutz, D. M. Tooke, A. L. Spek, F. Hartl, R. W. A. Havenith, G. P. M. van Klink, G. van Koten, *Inorg. Chem.* **2009**, *48*, 1887; c) S. K. Padhi, K. Tanaka, *Inorg. Chem.* **2011**, *50*, 10718; d) Y.-M. Zhang, J.-Y. Shao, C.-J. Yao, Y.-W. Zhong, *Dalton Trans.* **2012**, *41*, 9280.

[23] S. Ott, M. Borgström, L. Hammarström, O. Johansson, *Dalton Trans.* **2006**, 1434.

[24] S. Zhao, S. M. Arachchige, C. Slebodnick, K. J. Brewer, *Inorg. Chem.* **2008**, *47*, 6144.

[25] a) A. Juris, V. Balzani, S. Campagna, G. Denti, S. Serroni, G. Frei, H. U. Güdel, *Inorg. Chem.* **1994**, *33*, 1491; b) F. Puntoriero, S. Serroni, A. Licciardello, M. Venturi, A. Juris, V. Ricevuto, S. Campagna, *J. Chem. Soc. Dalton Trans.* **2001**, 1035; c) T. L. Easun, W. Z. Alsindi, M. Towrie, K. L. Ronayne, X.-Z. Sun, M. D. Ward, M. W. George, *Inorg. Chem.* **2008**, *47*, 5071; d) Y. Fan, L.-Y. Zhang, F.-R. Dai, L.-X. Shi, Z.-N. Chen, *Inorg. Chem.* **2008**, *47*, 2811.

[26] a) M. Kobayashi, S. Masaoka, K. Sakai, *Angew. Chem.* **2012**, *124*, 7549; *Angew. Chem. Int. Ed.* **2012**, *51*, 7431; b) M. Schulz, M. Karnahl, M. Schwalbe, J. G. Vos, *Coord. Chem. Rev.* **2012**, *256*, 1682.

[27] K. Nakamaru, *Bull. Chem. Soc. Jpn.* **1982**, *55*, 1639.

[28] G. M. Sheldrick, *Acta Crystallogr. Sect. A* **2008**, *64*, 112.

[29] O. V. Dolomanov, L. J. Bourhis, R. J. Gildea, J. A. K. Howard, H. Puschmann, *J. Appl. Crystallogr.* **2009**, *42*, 339.

[30] Gaussian 09 (Revision A.2), M. J. Frisch, G. W. Trucks, H. B. Schlegel, G. E. Scuseria, M. A. Robb, J. R. Cheeseman, J. A. Montgomery, Jr., T. Vreven, K. N. Kudin, J. C. Burant, J. M. Millam, S. S. Iyengar, J. Tomasi, V. Barone, B. Mennucci, M. Cossi, G. Scalmani, N. Rega, G. A. Petersson, H. Nakatsuji, M. Hada, M. Ehara, K. Toyota, R. Fukuda, J. Hasegawa, M. Ishida, T. Nakajima, Y. Honda, O. Kitao, H. Nakai, M. Klene, X. Li, J. E. Knox, H. P. Hratchian, J. B. Cross, C. Adamo, J. Jaramillo, R. Gomperts, R. E. Stratmann, O. Yazyev, A. J. Austin, R. Cammi, C. Pomelli, J. W. Ochterski, P. Y. Ayala, K. Morokuma, G. A. Voth, P. Salvador, J. J. Dannenberg, V. G. Zakrzewski, S. Dapprich, A. D. Daniels, M. C. Strain, O. Farkas, D. K. Malick, A. D. Rabuck, K. Raghavachari, J. B. Foresman, J. V. Ortiz, Q. Cui, A. G. Baboul, S. Clifford, J. Cioslowski, B. B. Stefanov, G. Liu, A. Liashenko, P. Piskorz, I. Komaromi, R. L. Martin, D. J. Fox, T. Keith, M. A. Al-Laham, C. Y. Peng, A. Nanayakkara, M. Challacombe, P. M. W. Gill, B. Johnson, W. Chen, M. W. Wong, C. Gonzalez, J. A. Pople, Gaussian, Inc., Wallingford CT, **2009**.

[31] a) T. H. Dunning, P. J. Hay in *Modern Theoretical Chemistry*, *Vol. 3* (Ed.: H. F. Schaefer), Plenum, New York, **1976**, p. 1; b) P. J. Hay, W. R. Wadt, *J. Chem. Phys.* **1985**, *82*, 270; c) W. R. Wadt, P. J. Hay, *J. Chem. Phys.* **1985**, *82*, 284; d) P. J. Hay, W. R. Wadt, *J. Chem. Phys.* **1985**, *82*, 299.

[32] a) A. D. Becke, *J. Chem. Phys.* **1993**, *98*, 5648; b) C. Lee, W. Yang, R. G. Parr, *Phys. Rev. B* **1988**, *37*, 785.

[33] a) A. Klamt, G. Schüürmann, *J. Chem. Soc. Perkin Trans. 2* **1993**, 799; b) J. Andzelm, C. Kölmel, A. Klamt, *J. Chem. Phys.* **1995**, *103*, 9312; c) V. Barone, M. Cossi, *J. Phys. Chem. A* **1998**, *102*, 1995; d) M. Cossi, N. Rega, G. Scalmani, V. Barone, *J. Comput. Chem.* **2003**, *24*, 669; e) Y. Takano, K. N. Houk, *J. Chem. Theory Comput.* **2005**, *1*, 70.

Received: March 12, 2013